analytical chemistry

Article

pubs.acs.org/ac

# Conjugated Polymer-Based Hybrid Materials for Turn-On Detection of $CO_2$ in Plant Photosynthesis

Hongbo Yuan,[†,§,∥] Yibing Fan,[‡,∥] Chengfen Xing,[*,‡] Ruimin Niu,[‡] Ran Chai,[†] Yong Zhan,[*,†] Junjie Qi,[‡] Hailong An,[‡] and Jialiang Xu[*,§]

[†]School of Materials Science and Engineering, Hebei University of Technology, Tianjin 300401, P.R. China

[‡]Institute of Biophysics, Hebei University of Technology, Tianjin 300401, P.R. China

[§]Institute for Molecules and Materials, Radboud University, Heyendaalseweg 135, 6525 AJ Nijmegen, The Netherlands

Supporting Information

**ABSTRACT:** Detection of carbon dioxide ($CO_2$) is of fundamental importance in diverse applications ranging from environmental analysis to agricultural production. In this work, a hybrid probe based on guanidinium-pendent oligofluorene (G-OF) and water-soluble conjugated polythiophene (PTP) has been developed for the turn on detection of $CO_2$ with low background signal, taking advantage of the efficient fluorescence quenching of the tight aggregate of **G-OF/PTP**. In the presence of $CO_2$, the electrostatic repulsion between G-OF and PTP can be effectively enhanced through protonation of the side chains, leading to the disaggregation and thus the "turn-on" fluorescence. The strategy allows for the light-up visible detection of $CO_2$ with high sensitivity. Importantly, this system is capable of sensitively monitoring the concentration changes of $CO_2$ in the process of the photosynthesis, which represents a concept to monitor the photosynthesis based on water-soluble conjugated polymers.

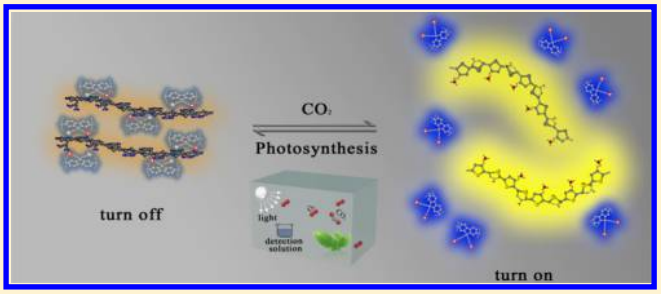


Carbon dioxide ($CO_2$) is a greenhouse gas contributing immeasurably to the global climate change and acts as an asphyxiant with the maximal acceptable concentration defined as 3.0%.[1−3] $CO_2$ also plays an essential role in plant photosynthesis. A total of 90−95% of the dry weight of plants derives from the assimilation of $CO_2$ during photosynthesis.[4,5] In this context, monitoring the photosynthesis of vegetation is not only crucial for raising the productivity of agriculture but also important for the better fixation of $CO_2$. Therefore, the detection of $CO_2$, in particular during the process of photosynthesis, is of great significance for global warming monitoring,[6,7] medical diagnosis,[8,9] and agricultural production.[10] Optical $CO_2$ detection methods have exhibited their advantages including convenience, low cost, and fastness, over the traditional analytical methodologies such as near-infrared spectroscopy,[11] gas chromatography/mass spectrometry,[12,13] and electrochemical techniques.[14] For example, several effective fluorescent probes based on aggregate-induced emission (AIE) have been recently developed for monitoring $CO_2$.[15−19] Yoon and coauthors realized colorimetric and fluorescent $CO_2$ detection by applying polydiacetylene in aqueous solution and in the solid state.[20] However, most of the established approaches have relatively high background fluorescence signal or require additional accessory molecules.[20] Moreover, to the best of our knowledge, very few examples of optical sensors have been reported to detect the changes of $CO_2$ in the process of photosynthesis, which is highly desirable.

Water-soluble conjugated polyelectrolytes are characterized by their delocalized $\pi$-electronic backbones and extraordinary light-harvesting capacities, exhibiting a signal amplification effect.[21−24] In the past few years, water-soluble conjugated polymers have been widely employed as an efficient platform for the detection of small molecules[25−27] and biomolecules such as DNA,[28−30] protein,[31−33] and enzymes,[34,35] with specificity and high sensitivity. They have been further developed into promising materials for broad biological applications in disease diagnosis,[36] drug screening and delivery,[37,38] cell imaging,[39] and antimicrobial susceptibility testing.[40−42] Inspired by these studies, we illustrate here a fluorescent, visible and "turn-on" detection system for $CO_2$ in dissolved and gaseous states as well as in plant photosynthesis, by hybridizing the guanidinium-pendent oligofluorene (G-OF) and water-soluble conjugated polymer poly(3-(2′-*N*,*N*-dipropanoic acid-ethylamino)-2,5-thiophene) (PTP). As illustrated in Scheme 1, PTP is designed to be functionalized with one amino group and two carboxylate groups in each repeat unit, while G-OF has guanidinium groups in the side chains. In the absence of $CO_2$, the guanidinium group of G-OF is partly protonated and the polymer exhibits positive charges, interacting with anionic PTP by tight electrostatic and $\pi-\pi$

**Received:** April 15, 2016
**Accepted:** June 2, 2016
**Published:** June 2, 2016





DOI: 10.1021/acs.analchem.6b01489
*Anal. Chem.* 2016, 88, 6593−6597

**Scheme 1. (a) Charge Changes of G-OF and PTP upon Bubbling with $CO_2$[a] and (b) Schematic Representation of G-OF/PTP Hybrid Probe for $CO_2$ Detection in Plant Photosynthesis[b]**

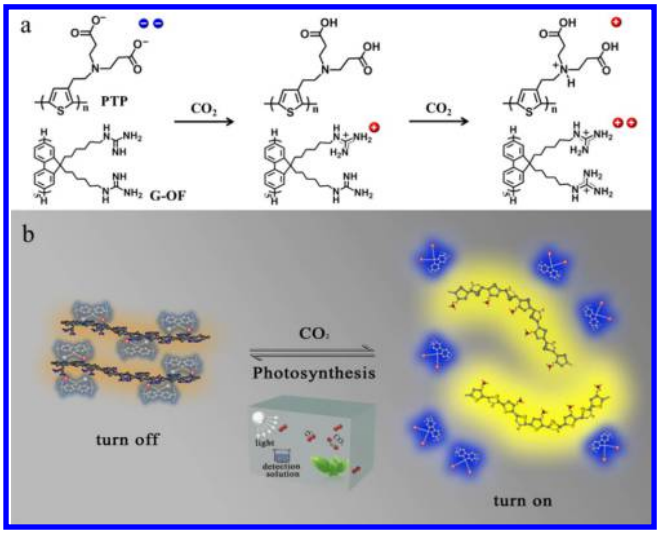


[a]The charge changes of G-OF and PTP according to the different p$K_a$ values of each side chain, the guanidinium, tertiary amine and carboxyl groups with p$K_a$ values of 13.6, 9.54, and 2.2, respectively.[43,44] [b]The fluorescence of both polymers is quenched upon the formation of the tight aggregate of **G-OF/PTP** but gets efficiently recovered in the presence of $CO_2$.

stacking interactions, forming micrometer-sized supramolecularly assembled aggregates. These strong supramolecular interactions dramatically quenches (turn-off) the fluorescence of both polymers. When $CO_2$ is bubbled into the solution, the guanidinium groups of G-OF are completely protonated and the polymers become positively charged. At the same time, both the amino and the carboxyl groups of PTP are protonated, endows the polymer also with positive charges. Thus, the electrostatic repulsion between G-OF and PTP dominates and leads to the break of the **G-OF/PTP** aggregates, resulting in the fluorescence recovery of G-OF and PTP (turn-on). The system is so sensitive that it can be effectively applied to monitor the concentration changes of $CO_2$ in the process of plant photosynthesis, which continuously converts $CO_2$ into carbohydrate by the assimilation of sunlight and $H_2O$ and converts.[45,46] The fluorescence of **G-OF/PTP** is gradually quenched as the plant photosynthesis is consuming the $CO_2$. Furthermore, the $CO_2$ detection can be visualized directly in view of color changes of **G-OF/PTP** in aqueous medium under UV light.

## EXPERIMENTAL SECTION

**Materials and Measurements.** G-OF and PTP were synthesized referring to the procedure reported in the literature.[44,47] All chemicals were purchased from Acros, Aladdin, or Alfa Aesar and used as received if not specially stated. All organic solvent were purchased from Tianjin Guangfu Ltd. $CO_2$, $N_2$, and $O_2$ were certified food grade (99.99% purity) and obtained from Tianjin Lianbo Ltd. All solutions were prepared with precooling Milli-Q water at 4 °C. The fluorescence spectra were taken on a Hitachi F-4500 fluorimeter equipped with a xenon lamp excitation source at 4 °C which was controlled by recirculating chiller F-305 (BÜCHI). Dynamic light scattering (DLS) experiments and $\zeta$ potentials were carried out on Nano-S90 (Malvern Instruments, U.K.).

**Detection of $CO_2$ in Water.** To 400.0 $\mu$L of dd$H_2O$ was added G-OF (0.8 $\mu$M) and bubbled with different volumes of $CO_2$ at a constant flow rate of 1.5 mL/min, and then 875.0 nM (in repeat units) of PTP was added and mixed gently. After 5.0 min of incubation, the fluorescence spectra were measured in quartz cuvettes by applying a Hitachi F-4500 fluorimeter at 4 °C. The excitation wavelength was 378 nm.

**Preparation for Different Ratios of $CO_2$/ $N_2$ Mixtures.** The flow rate of $CO_2$ and $N_2$ were controlled by standard flowmeter and mixed in a sampling bag.

**Detection of $CO_2$ by Composite Film.** G-OF solution (10.0 $\mu$M) was sprayed on the cellulose ester film. After 5.0 min of exposure to a $CO_2$ atmosphere, the PTP (8.0 $\mu$M) was sprayed, and then the images were taken under UV light ($\lambda$ = 365 nm).

**Detection of $CO_2$ in Photosynthesis.** An airtight chamber (500 × 500 × 500 $mm^3$) was designed with an inlet, an outlet, lamps (300 W), and a delivery window. *Zea mays* were grown in vermiculite for 14 days in a greenhouse. We eliminated the air in chamber through the method of vacuum and then filled with $CO_2$ to 1.0 atm. The 1.0 mL of detection solution contained with G-OF ([G-OF] = 0.8 $\mu$M) was put in the chamber after different time of illumination. After 12 h of equilibrium, 875.0 nM (in repeat units) of PTP was added, and the fluorescence spectra were measured.

## RESULTS AND DISCUSSION

PTP and G-OF were synthesized referring to the reported procedures.[44,47] The detection of $CO_2$ by the **G-OF/PTP** hybrid probe is based on the efficient fluorescence quenching of both polymers. G-OF emits bright blue light in aqueous solution with the fluorescence spectrum maximized at 420 nm, while PTP emits yellow fluorescence with a maximum at 560 nm. The fluorescence of G-OF ([G-OF] = 0.8 $\mu$M) was quenched upon addition of PTP ([PTP] = 0–875.0 nM in repeat units) in water. As shown in Figure 1a, the emission of

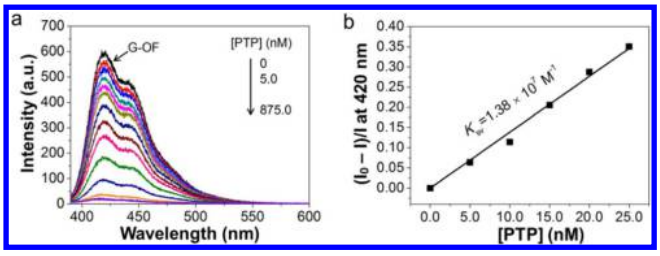


**Figure 1.** (a) Fluorescence spectra of G-OF in water with successive additions of PTP. (b) $K_{SV}$ plot of G-OF in the presence of PTP. [G-OF] = 0.8 $\mu$M, [PTP] = 0–875.0 nM (in repeat units). $I$ and $I_0$ represent the emission intensity of G-OF at 420 nm in the presence and absence of PTP. Measurements were performed at 4 °C in sterile water. The excitation wavelength was 378 nm.

G-OF was decreased gradually with successive addition of PTP and the fluorescence of G-OF was efficiently quenched by 97.2% in the presence of PTP ([PTP] = 875.0 nM). The quenching efficiency was calculated by measuring the fluorescent changes of G-OF via the Stern–Volmer equation (eq 1):[48]

$$I_0/I = 1 + K_{SV}[Q] \quad (1)$$



DOI: 10.1021/acs.analchem.6b01489
*Anal. Chem.* 2016, 88, 6593–6597

The Stern−Volmer constant ($K_{SV}$) value was deduced to be $1.38 \times 10^7$ $M^{-1}$ from the linear Stern−Volmer plot with low concentrations of PTP (0−25.0 nM) (Figure 1b), indicating the superquenching of G-OF by PTP. The intense electrostatic and $\pi-\pi$ stacking interactions between G-OF and PTP were attributed to drive the formation of the tight aggregation of **G-OF/PTP** complex and to induce the superquenching behavior.

The sensitivity of the assembled **G-OF/PTP** complex to $CO_2$ was first examined in the solution state, by bubbling $CO_2$ into the aqueous solution of G-OF in the presence of PTP and the results are summarized in Figure 2. As shown in Figure 2a,

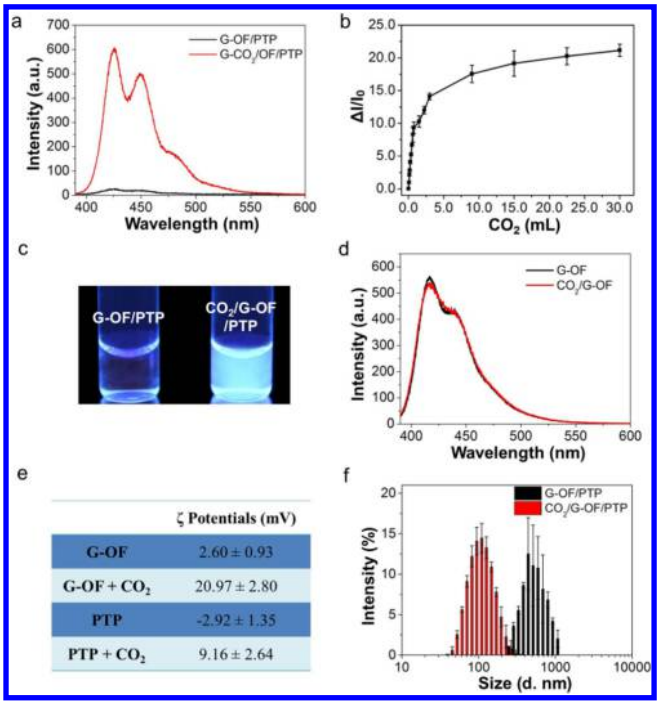


**Figure 2.** (a) Fluorescence spectra of G-OF in the presence of PTP with and without $CO_2$. (b) Fluorescence intensity of G-OF at 420 nm in the presence of PTP after bubbling with different volumes of $CO_2$ in water at 4 °C. $I_0$ and $I$ represent the emission intensity of G-OF at 420 nm in the presence of PTP without and with $CO_2$, respectively, and $\Delta I/I_0$ is equal to $(I - I_0)/I_0$. All data were presented as mean values ± standard deviation of three separate experiments. Error bars represent standard deviations of data from three separate measurements. (c) Fluorescence images of G-OF in the presence of PTP in water with and without $CO_2$, under UV light excitation ($\lambda$ = 365 nm). (d) Emission spectra of G-OF in water with and without $CO_2$. (e) $\zeta$ Potentials of G-OF and PTP with and without $CO_2$ in water. (f) Size distribution histograms of G-OF in the presence of PTP with and without $CO_2$ resulting from dynamic light scattering measurement. [G-OF] = 0.8 $\mu$M, [PTP] = 875.0 nM (in repeat units), the bubbling volumes of $CO_2$ increase from 0 to 30.0 mL at a constant flow rate of 1.5 mL/min. Measurements were performed at 4 °C in sterile water. The excitation wavelength was 378 nm.

the emission intensity of G-OF has been recovered by approximately 20 times after reacting with $CO_2$. The recovery rate is dependent on the bubbling volumes of $CO_2$. As shown in Figure 2b, the fluorescence intensity of **G-OF/PTP** at 420 nm increases with the amount of $CO_2$ bubbled and the detection limit can be as lower as 75.0 $\mu$L. Importantly, the detection of $CO_2$ can be directly visualized through the color changes of **G-OF/PTP** from dark blue to bright blue under UV irradiation upon bubbling with $CO_2$, as shown in the images in Figure 2c. Control experiments were carried out to check the effect of $CO_2$ on the emitting behaviors of G-OF and PTP. $CO_2$ was found to induce very little effect on the emission spectra of G-OF in the absence of PTP (Figure 2d), while the emission of PTP was decreased with the addition of $CO_2$ (see Figure S3 in the Supporting Information). This is consistent with the working mechanism proposed in Scheme 1, where the net charges of PTP is decreased and the dominating interchain $\pi-\pi$ stacking leads to the formation of aggregates and results in the self-quenching of PTP, with the increasing amount of $CO_2$.[49,50]

The $\zeta$ potentials provide further evidence for the interactions between G-OF and PTP in the presence and absence of $CO_2$ (Figure 2e). $\zeta$ potentials of G-OF and PTP became more positive upon reaction with $CO_2$ because the guanidinium groups of G-OF and the amino and carboxylate groups of PTP became completely protonated. Additionally, the dynamic light scattering (DLS) measurements were also conducted. As shown in Figure 2f, the average hydrodynamic radius of **G-OF/PTP** aggregates is 842.2 nm, which is much larger than that in the presence of $CO_2$ (104.1 nm). This is a direct indication that the **G-OF/PTP** aggregates were separated due to the electrostatic repulsion between G-OF and PTP. In order to further study the mechanism of our system, the fluorescence recovery of the hybrid probe **G-OF/PTP** with other gases in water was measured. As illustrated in Figure S4 in the Supporting Information, no fluorescence recovery was produced by $N_2$ or $O_2$, indicating little interference from other gases in atmosphere. Moreover, the interference of $SO_2$ was checked as well. As illustrated in Figure S5, the emission of **G-OF/PTP** cannot be recovered in the presence of $SO_2$, possibly resulting from the total quenching of G-OF by $SO_2$ which is different from that in the presence of $CO_2$. Therefore, these results demonstrate a fluorescent, visible, and turn-on detection for $CO_2$ with high sensitivity and selectivity.

Taking the practicality into consideration, $CO_2$ is always present in the atmosphere and acts as an asphyxiant. Therefore, the fluorescence spectra of the **G-OF/PTP** hybrid probe before and after bubbling with $CO_2/N_2$ with different ratios were examined. As illustrated in Figure 3, the emission was recovered gradually with the increasing ratio of $CO_2$ in a series of $CO_2/N_2$ mixtures and the detected minimum ratio of $CO_2$ was 1.0% (Figure 3b). In practical terms, the maximal acceptable concentration was defined under 3.0%.[3] Furthermore, the hybrid probe **G-OF/PTP** was also applied for solid-state

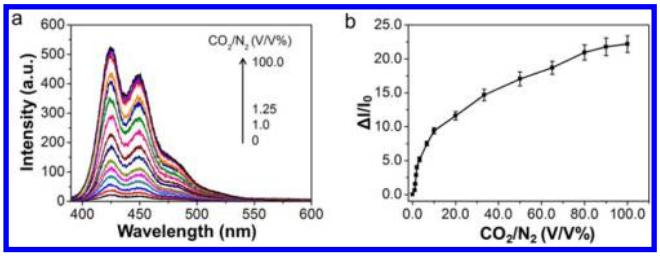


**Figure 3.** (a) Fluorescence spectra of G-OF in the presence of PTP before and after bubbling with $CO_2/N_2$ mixtures with different ratios for 2 min at a constant flow rate of 1.5 mL/min. (b) Plot of the fluorescence intensity of G-OF at 420 nm in the presence of PTP as a function of the ratio of $CO_2$ in $CO_2/N_2$ mixtures. [G-OF] = 0.8 $\mu$M, [PTP] = 875.0 nM (in repeat units), the volume ratios of $CO_2/N_2$ change from 0 to 100.0%. Error bars represent standard deviations of data from three separate measurements. Measurements were performed at 4 °C in water. The excitation wavelength was 378 nm.



DOI: 10.1021/acs.analchem.6b01489
Anal. Chem. 2016, 88, 6593−6597

sensing of $CO_2$. **G-OF/PTP** was sprayed onto a substrate of the cellulose ester film, and a dark blue to bright blue color change was observed under UV light upon exposure to $CO_2$ atmosphere (see Figure S6 in the Supporting Information). Therefore, our probe system offers a $CO_2$ detection approach allows for the assessment of the asphyxial risk.

Furthermore, the **G-OF/PTP**-based detection for $CO_2$ in gaseous phase was studied in confined spaces. As shown in Figure 4a, the detection solution of G-OF in water was placed

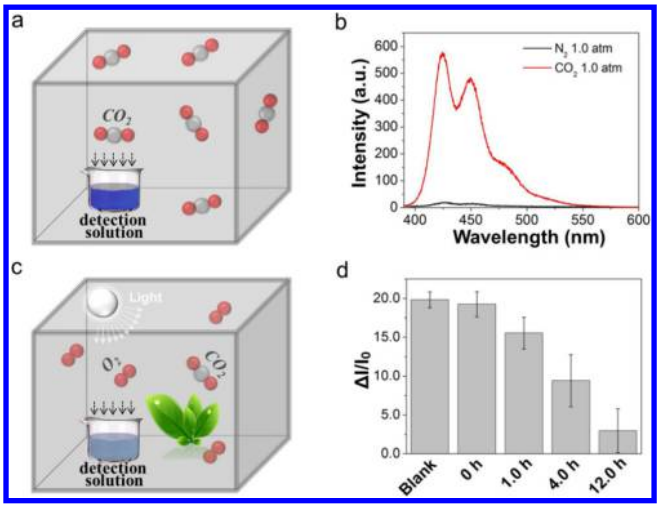


**Figure 4.** Scheme (a) and fluorescence spectra (b) of the G-OF with $N_2$ and $CO_2$ atmosphere in the presence of PTP. Scheme (c) and fluorescence intensities (d) of G-OF in $CO_2$ atmosphere in the presence of PTP versus different time of illumination. Blank represents the fluorescence intensities of G-OF in the presence of PTP in $CO_2$ atmosphere without photosynthesis. All data were presented as mean values ± standard deviation of three separate experiments. Error bars represent standard deviations of data from three separate measurements. [G-OF] = 0.8 $\mu$M, [PTP] = 875.0 nM (in repeat units). Measurements were performed at 4 °C in water. The excitation wavelength was 378 nm.

in a confined chamber with $CO_2$ atmosphere (1.0 atm) for 12 h, and then the emission spectra of the **G-OF/PTP** hybrid probe was measured. Figure 4b exhibits that the gaseous $CO_2$ induces the significant recovery of emission through the absorption to the detection solution. Additionally, the different volume ratios of $CO_2/N_2$ mixtures in confined spaces were also detected, and the detected minimum ratio of $CO_2$ was 1.0% as well (see Figure S7 in the Supporting Information). In this way, the **G-OF/PTP**-based system allows for the detection of the gaseous $CO_2$ in confined spaces, which is extremely important for the workers in closed spaces to avoid the risk of asphyxia.

Finally, the $CO_2$ was monitored in the process of photosynthesis. It is well-known that plant photosynthesis converts $CO_2$ into carbohydrate by assimilation of sunlight and $H_2O$. Here, we employed *Zea mays*, a $C_4$-photosynthetic plant with high photosynthetic rate,[51,52] as a model system to study the response of the **G-OF/PTP**-based probe to monitor the $CO_2$ changes in plant photosynthesis. As exhibited in Figure 4c, *Zea mays* was placed in the confined chamber with light and $CO_2$, and the fluorescence intensity of the **G-OF/PTP** hybrid probe was decreased gradually with the increase of the illumination time (Figure 4d), indicating the assimilation of $CO_2$ by photosynthesis. Therefore, our $CO_2$ detection strategy can be applied to monitor $CO_2$ changes in plant photosynthesis.

## CONCLUSIONS

In summary, we have designed a hybrid probe comprising guanidinium-pendent oligofluorene (G-OF) and water-soluble conjugated polythiophene derivative (PTP) for sensing $CO_2$ with very low background signal. This detection strategy takes advantage of the superquenching property of G-OF by PTP in the tight aggregates of **G-OF/PTP**, and the $CO_2$ controlled aggregation induces the turn-on signal of fluorescence. The new, simple, and light-up visible $CO_2$ assay system has several unique characteristics. First, the **G-OF/PTP**-based hybrid probe realizes the quantitative detection of $CO_2$ in both gaseous and dissolved phase. Second, the strategy can be applied for assessment of asphyxial risk in confined spaces. Furthermore, our $CO_2$ optical detection system enables the monitoring of $CO_2$ in plant photosynthesis. Therefore, the **G-OF/PTP**-based turn-on approach for $CO_2$ detection provides meaningful applications in asphyxia diagnosis and monitoring plant photosynthesis.

## ASSOCIATED CONTENT

### Supporting Information

The Supporting Information is available free of charge on the ACS Publications website at DOI: 10.1021/acs.analchem.6b01489.

Comparison of the strategies of "pre-mixing" ($CO_2$ was first mixed with G-OF) and "post-mixing" ($CO_2$ was first mixed with PTP); the fluorescence recovery of the hybrid probe G-OF/PTP with other gases; and detection of $CO_2$ by composite film and additional spectral figures (PDF)

## AUTHOR INFORMATION

### Corresponding Authors

*E-mail: xingc@hebut.edu.cn. Fax: +86 (0)22 60435642.
*E-mail: zhan_yong2014@163.com. Fax: +86 (0)22 60438468.
*E-mail: xujialiang@science.ru.nl. Fax: +31 (0) 24 36 53393.

### Author Contributions

‖H.Y. and Y.F. contributed equally.

### Notes

The authors declare no competing financial interest.

## ACKNOWLEDGMENTS

We are grateful for the financial supports from the National Natural Science Foundation of China (Grant No. 21574037), the "100 Talents" Program of Hebei Province, China (Grant No. E2014100004), the Program for Excellent Innovative Talents in Universities of Hebei Province, China (Grant No. BJ2014011), the Natural Science Foundation of Hebei Province (Grant No. B2015202330), the Tianjin Natural Science Foundation (Grant No. 15JCYBJC17500), and The Netherlands Organization for Scientific Research (NWO) with the Veni Grant (Grant No. 680-47-437). The authors acknowledge Prof. Shu Wang (Institute of Chemistry, Chinese Academy of Sciences) for valuable suggestions on this work.

## REFERENCES

(1) Cox, P. M.; Betts, R. A.; Jones, C. D.; Spall, S. A.; Totterdell, I. J. *Nature* **2000**, *408*, 184−187.



DOI: 10.1021/acs.analchem.6b01489
*Anal. Chem.* 2016, 88, 6593−6597

(2) Leaf, D.; Verolme, H. J.; Hunt, W. F. *Environ. Int.* **2003**, *29*, 303−310.
(3) Guais, A.; Brand, G.; Jacquot, L.; Karrer, M.; Dukan, S.; Grévillot, G.; Molina, T. J.; Bonte, J.; Regnier, M.; Schwartz, L. *Chem. Res. Toxicol.* **2011**, *24*, 2061−2070.
(4) Bassham, J. A. *Science* **1977**, *197*, 630−638.
(5) Zelitch, I. *Proc. Natl. Acad. Sci. U. S. A.* **1973**, *70*, 579−586.
(6) Gillett, N. P.; Arora, V. K.; Matthews, D.; Allen, M. R. *J. Clim.* **2013**, *26*, 6844−6858.
(7) Frölicher, T. L.; Winton, M.; Sarmiento, J. L. *Nat. Clim. Change* **2013**, *4*, 40−44.
(8) Hassan, M. I.; Shajee, B.; Waheed, A.; Ahmad, F.; Sly, W. S. *Bioorg. Med. Chem.* **2013**, *21*, 1570−1582.
(9) Geers, C.; Gros, G. *Physiol. Rev.* **2000**, *80*, 681−715.
(10) Gray, J. M.; Frolking, S.; Kort, E. A.; Ray, D. K.; Kucharik, C. J.; Ramankutty, N.; Friedl, M. A. *Nature* **2014**, *515*, 398−401.
(11) Neethirajan, S.; Jayas, D.; Sadistap, S. *Food Bioprocess Technol.* **2009**, *2*, 115−121.
(12) Amao, Y.; Nakamura, N. *Sens. Actuators, B* **2005**, *107*, 861−865.
(13) Oter, O.; Ertekin, K.; Derinkuyu, S. *Talanta* **2008**, *76*, 557−563.
(14) Dansby-Sparks, R. N.; Jin, J.; Mechery, S. J.; Sampathkumaran, U.; Owen, T. W.; Yu, B. D.; Goswami, K.; Hong, K.; Grant, J.; Xue, Z.-L. *Anal. Chem.* **2010**, *82*, 593−600.
(15) Wang, H.; Chen, D.; Zhang, Y.; Liu, P.; Shi, J.; Feng, X.; Tong, B.; Dong, Y. *J. Mater. Chem. C* **2015**, *3*, 7621−7626.
(16) Liu, Y.; Tang, Y.; Barashkov, N. N.; Irgibaeva, I. S.; Lam, J. W.; Hu, R.; Birimzhanova, D.; Yu, Y.; Tang, B. Z. *J. Am. Chem. Soc.* **2010**, *132*, 13951−13953.
(17) Ali, R.; Lang, T.; Saleh, S. M.; Meier, R. J.; Wolfbeis, O. S. *Anal. Chem.* **2011**, *83*, 2846−2851.
(18) Ishida, M.; Kim, P.; Choi, J.; Yoon, J.; Kim, D.; Sessler, J. L. *Chem. Commun.* **2013**, *49*, 6950−6952.
(19) Suresh, V. M.; Bonakala, S.; Roy, S.; Balasubramanian, S.; Maji, T. K. *J. Phys. Chem. C* **2014**, *118*, 24369−24376.
(20) Xu, Q.; Lee, S.; Cho, Y.; Kim, M. H.; Bouffard, J.; Yoon, J. *J. Am. Chem. Soc.* **2013**, *135*, 17751−17754.
(21) Feng, L.; Zhu, C.; Yuan, H.; Liu, L.; Lv, F.; Wang, S. *Chem. Soc. Rev.* **2013**, *42*, 6620−6633.
(22) Rochat, S.; Swager, T. M. *J. Am. Chem. Soc.* **2013**, *135*, 17703−17706.
(23) Wasilke, J.-C.; Obrey, S. J.; Baker, R. T.; Bazan, G. C. *Chem. Rev.* **2005**, *105*, 1001−1020.
(24) Jo, J.; Pouliot, J. R.; Wynands, D.; Collins, S. D.; Kim, J. Y.; Nguyen, T. L.; Woo, H. Y.; Sun, Y.; Leclerc, M.; Heeger, A. J. *Adv. Mater.* **2013**, *25*, 4783−4788.
(25) Liu, J.; Yee, K.-K.; Lo, K. K.-W.; Zhang, K. Y.; To, W.-P.; Che, C.-M.; Xu, Z. *J. Am. Chem. Soc.* **2014**, *136*, 2818−2824.
(26) Xing, C.; Yuan, H.; Xu, S.; An, H.; Niu, R.; Zhan, Y. *ACS Appl. Mater. Interfaces* **2014**, *6*, 9601−9607.
(27) Jia, Y.; Zuo, X.; Lou, X.; Miao, M.; Cheng, Y.; Min, X.; Li, X.; Xia, F. *Anal. Chem.* **2015**, *87*, 3890−3894.
(28) Ho, H. A.; Boissinot, M.; Bergeron, M. G.; Corbeil, G.; Dore, K.; Boudreau, D.; Leclerc, M. *Angew. Chem., Int. Ed.* **2002**, *41*, 1548−1551.
(29) Liu, X.; Ouyang, L.; Cai, X.; Huang, Y.; Feng, X.; Fan, Q.; Huang, W. *Biosens. Bioelectron.* **2013**, *41*, 218−224.
(30) Xing, X.-J.; Liu, X.-G.; He, Y.; Lin, Y.; Zhang, C.-L.; Tang, H.-W.; Pang, D.-W. *Biomacromolecules* **2013**, *14*, 117−123.
(31) Usmani, S. M.; Zirafi, O.; Muller, J. A.; Sandi-Monroy, N. L.; Yadav, J. K.; Meier, C.; Weil, T.; Roan, N. R.; Greene, W. C.; Walther, P.; Nilsson, K. P. R.; Hammarstrom, P.; Wetzel, R.; Pilcher, C. D.; Gagsteiger, F.; Faendrich, M.; Kirchhoff, F.; Munch, J. *Nat. Commun.* **2014**, *5*, 1962−1968.
(32) Yuan, H.; Xing, C.; An, H.; Niu, R.; Li, R.; Yan, W.; Zhan, Y. *ACS Appl. Mater. Interfaces* **2014**, *6*, 14790−14794.
(33) Yuan, H.; Qi, J.; Xing, C.; An, H.; Niu, R.; Zhan, Y.; Fan, Y.; Yan, W.; Li, R.; Wang, B. *Adv. Funct. Mater.* **2015**, *25*, 4412−4418.
(34) Kumaraswamy, S.; Bergstedt, T.; Shi, X.; Rininsland, F.; Kushon, S.; Xia, W.; Ley, K.; Achyuthan, K.; McBranch, D.; Whitten, D. *Proc. Natl. Acad. Sci. U. S. A.* **2004**, *101*, 7511−7515.
(35) Bai, J.; Liu, C.; Yang, T.; Wang, F.; Li, Z. *Chem. Commun.* **2013**, *49*, 3887−3889.
(36) Yang, Q.; Dong, Y.; Wu, W.; Zhu, C.; Chong, H.; Lu, J.; Yu, D.; Liu, L.; Lv, F.; Wang, S. *Nat. Commun.* **2012**, *3*, 1206.
(37) Lee, S. H.; Kang, Y. Y.; Jang, H.-E.; Mok, H. *Adv. Drug Delivery Rev.* **2015**, DOI: 10.1016/j.addr.2015.10.009.
(38) Shi, H.; Kwok, R. T.; Liu, J.; Xing, B.; Tang, B. Z.; Liu, B. *J. Am. Chem. Soc.* **2012**, *134*, 17972−17981.
(39) Lee, K.; Lee, J.; Jeong, E. J.; Kronk, A.; Elenitoba-Johnson, K. S.; Lim, M. S.; Kim, J. *Adv. Mater.* **2012**, *24*, 2479−2484.
(40) Bai, H.; Yuan, H.; Nie, C.; Wang, B.; Lv, F.; Liu, L.; Wang, S. *Angew. Chem., Int. Ed.* **2015**, *54*, 13208−13213.
(41) Li, R.; Niu, R.; Qi, J.; Yuan, H.; Fan, Y.; An, H.; Yan, W.; Li, H.; Zhan, Y.; Xing, C. *ACS Appl. Mater. Interfaces* **2015**, *7*, 14569−14572.
(42) Yan, W.; Yuan, H.; Li, R.; Fan, Y.; Zhan, Y.; Qi, J.; An, H.; Niu, R.; Li, G.; Xing, C. *Macromol. Chem. Phys.* **2015**, *216*, 1603−1608.
(43) Shimada, N.; Nakayama, M.; Kano, A.; Maruyama, A. *Biomacromolecules* **2013**, *14*, 1452−1457.
(44) Chen, H.; Wang, B.; Zhang, J.; Nie, C.; Lv, F.; Liu, L.; Wang, S. *Chem. Commun.* **2015**, *51*, 4036−4039.
(45) Moroney, J. V.; Jungnick, N.; DiMario, R. J.; Longstreth, D. J. *Photosynth. Res.* **2013**, *117*, 121−131.
(46) Busch, F. A.; Sage, T. L.; Cousins, A. B.; Sage, R. F. *Plant, Cell Environ.* **2013**, *36*, 200−212.
(47) Xing, C.; Xu, Q.; Tang, H.; Liu, L.; Wang, S. *J. Am. Chem. Soc.* **2009**, *131*, 13117−13124.
(48) Kim, O.-K.; Je, J.; Melinger, J. S. *J. Am. Chem. Soc.* **2006**, *128*, 4532−4533.
(49) Yuan, H.; Xing, C.; Xu, J. unpublished results.
(50) To demonstrate the interactions involved for the $CO_2$ sensing, the strategies of "pre-mixing" ($CO_2$ was first mixed with G-OF) and "post-mixing" ($CO_2$ was first mixed with PTP) were compared. As shown in Figure S1 (Supporting Information), the fluorescence can be recovered by $CO_2$ whether $CO_2$ was premixed with G-OF or PTP. However, when G-OF was first mixed with PTP and then $CO_2$ was introduced, no subsequent emission recovery was produced (see Figure S2 in the Supporting Information). Therefore, in our approach, the G-OF was first premixed with $CO_2$ for 5.0 min at 4 °C, and then PTP was added to the solution.
(51) Marino, B. D.; McElroy, M. B. *Nature* **1991**, *349*, 127−131.
(52) Crespo, H.; Frean, M.; Cresswell, C.; Tew, J. *Planta* **1979**, *147*, 257−263.


DOI: 10.1021/acs.analchem.6b01489
*Anal. Chem.* 2016, 88, 6593−6597